The Effects of Climate Change on
Tradeoffs Among Forest Ecosystem Services

Nicholas D. C. Kullman

A thesis
submitted in partial fulfillment of the
requirements for the degree of

Master of Science

University of Washington

2016

Committee:

Sándor F. Tóth, Chair

David Butman

W. Art Chaovalitwongse

Program Authorized to Offer Degree:
Quantitative Ecology and Resource Management

University of Washington

Abstract

The Effects of Climate Change on
Tradeoffs Among Forest Ecosystem Services

Nicholas D. C. Kullman

Chair of the Supervisory Committee:
Associate Professor Sándor F. Tóth
School of Environmental and Forest Sciences

DRAFT

Forests provide a bounty to humans through ecosystem services such as wildlife habitat, recreation, and water and air purification. Forest managers seek to maximize the provision of ecosystem services and often do so for multiple ecosystem services simultaneously. While many studies predict that climate change will impact forests' ability to provide ecosystem services, no research has addressed the question of how climate change will impact the joint provision of ecosystem services. I address this question here in an attempt to better understand how the relationships between ecosystem services will change with climate. For example, how much additional fire hazard must be assumed in order to maintain an amount of habitat for a particular species. To study this question, I consider the growth of a forested area in the Deschutes National Forest under three climate scenarios of varying intensity. This area provides three competing ecosystem services whose joint provision is assessed under each of the climate scenarios: northern spotted owl habitat, water quality, and resistance to wildfire.

I find that ...

TABLE OF CONTENTS

LIST OF FIGURES

LIST OF TABLES

GLOSSARY

CLIMATE PROJECTION: The IPCC defines a climate projection as a model-derived estimate of future climate. *See* CLIMATE SCENARIO[56].

CLIMATE SCENARIO: The IPCC defines a scenario as a coherent, internally consistent and plausible description of a possible future state of the world. Herein, I use this term interchangeably with CLIMATE PROJECTION, since climate projections often underlie climate scenarios [56].

CLUSTER: Here, a set of contiguous forest stands whose combined area exceeds 200 ha

ECOSYSTEM SERVICE: Benefits that people receive from ecosystems, divided into four categories: supporting, provisioning, regulating and cultural [5]. Examples include food, soil formation, water purification, carbon storage, recreation, and education.

PARETO EFFICIENT: A solution to a multi-objective mathematical program is said to be Pareto efficient if no component of the solution can be improved without compromising at least one other component.

STAND DENSITY INDEX (SDI): Reineke's Stand Density Index is a measure of the stocking of a forest stand. See [61].

TRADEOFF: The sacrifice of achievement in one objective in order to achieve more in another.

ACKNOWLEDGMENTS

DRAFT

Thank you to all who contributed to my earning this degree.

DEDICATION

DRAFT

To ma femme and my family

Chapter 1

MEASURING CONFLICT IN MULTI-OBJECTIVE OPTIMIZATION: A CASE STUDY OF THE IMPACT OF CLIMATE CHANGE ON THE JOINT PROVISION OF FOREST ECOSYSTEM SERVICES

1.1 Introduction

Many problems are multi-objective. Building aircraft requires attention to weight, price, AND SOME OTHER STUFF CITE. Hospitals seek to maximize patient care, number of patients seen, and minimize cost CITE. Forest managers aim to provide carbon sequestration, wildlife habitat, recreation, timber revenues, and protection from wildfire. Designing cars involves attention to objectives like horsepower, price, luxury, and fuel economy. Daily, we all try to maximize our own objective functions involving work, social interaction, fitness and others.

Often, the objectives in these problems will conflict. When designing aircraft, as you decrease the weight, you drive price up. When hospitals maximize individual patient care, they are unable to see as many total patients. Forest managers increasing sequestered carbon drive up the severity of wildfires. Car manufacturers must generally sacrifice either price or luxury. We can only spend so many hours with friends and family and still keep our jobs.

To take full advantage of the resources at our disposal, optimal application of those resources is required. That is, understanding the balance between objectives let's you make better decisions. What if you adding just a bit of weight to the aircraft cut cost substantially? What if sacrificing just a bit of timber revenue entailed a huge increase in habitat for some species? Shaving off .1 seconds on the quarter-mile time on a new car only cost a hundredth of an mpg in the car you're building? For a decision maker to make the best decision, he or

she must know the best compromises at their disposal. They must know if a solution exists that makes drastic improvements with minimal sacrifice. This requires an understanding of the conflicting relationships among the objectives.

Numerous methods exist to attempt to quantify these conflicting relationships CITE. Some measures capture holistic conflict HYPERVOL/EPSILON ERROR. These are important and useful. Often we want more detail on pairwise conflict too. Other measures exist to provide the decision maker with the ability to drill down into this. However, the motivation for these pairwise methods is almost always the elimination of objectives from complex, many-objective problems in order to make them more computationally tractable. For these methods, In our pursuit of better computational performance, we lost sight of why we have to deal with these problems in the first place: conflicting management objectives. We argue that no current pairwise conflict metric adequately measures conflict to answer questions regarding objective relationships.

Perhaps the most commonly used pairwise conflict metric, PEARSON, fails to detect the absence of conflict as many studies have defined it (mono inc). For instance if objs look like THIS GRAPH?, it fails to distinguish between the two. The SPEARMAN AND KENDALL and other commonly used rank-based metrics also fail to distinguish between those two scenarios. WHAT ABOUT MUTUAL INFO? Zitzler's delta error is a more nuanced indicator of conflict, but it does not provide a means of pair-wise objective comparison, is computationally complex, and is focused on relative relationships of objs and does not consider objective achievement.

We propose here a new pairwise conflict metric that addresses all of the issues described. It accurately detects the lack of conflict, is capable of handling non-linear correlation, is computationally simple, and considers objective achievement rather than just achievement relative to one another.

We demonstrate this new metric's use on a multi-objective case study in the Deschutes National Forest. We also provide a consolidated discussion of conflict metrics for use in exact multi-objective optimization. This includes a discussion of Pareto frontier comparisons and

how to interpret them for the sake of guidance to decision makers, not just for algorithm comparison.

We define terms and layout notation first. Then we introduce the case study. Then we detail the results of the case study and the application of the metrics used here, both new and existing. And we conclude with closing remarks and a summary.

1.2 Methods

Bundled ecosystem services conflict with one another, and I argue that understanding the change in this conflict over time will enable forest planners to make more informed management decisions. Here, I provide formal definitions of what it means for ecosystem services to conflict, how to measure changes in conflict, and how a change in conflict impacts trade-off relationships.

1.2.1 Terminology

To aid in the discussion of conflict and trade-offs, I first present the definitions and notation used here.

The multi-objective problem   Consider the M-objective optimization problem

Maximize

$$\mathbf{f} = [f_1(\mathbf{x}), f_2(\mathbf{x}), \ldots, f_M(\mathbf{x})] \tag{1.1}$$

subject to

$$\mathbf{x} \in X \tag{1.2}$$

with *objective functions* $f_i(\mathbf{x}), i \in \{1, \ldots, M\}$ and feasible *decision vectors* (or *solutions*) $\mathbf{x} \in \mathbb{R}^n$ where n is the number of decision variables in the optimization problem. A set of equality and inequality constraints determine the *feasible decision space* X. Solutions in X are referenced by a superscript: $X = \{\mathbf{x}^1, \mathbf{x}^2, \ldots, \mathbf{x}^{|X|}\}$. Each objective function $f_i : \mathbb{R}^n \mapsto \mathbb{R}$ maps decision vectors to scalars in $\mathbb{R}$. The vector objective function $\mathbf{f} : X \mapsto \mathbb{R}^M$ maps the

feasible decision space to the *objective space* $\mathbb{R}^M$. The set of all objective functions is the *objective set* $\mathcal{M} = \{f_1, \ldots, f_M\}$.

Dominance and frontiers   A solution $\mathbf{x}^1$ is said to *dominate* another solution $\mathbf{x}^2$ ($\mathbf{x}^1 \succ \mathbf{x}^2$) if

$$\exists f_i \in \mathcal{M} : f_i(\mathbf{x}^1) > f_i(\mathbf{x}^2) \text{ and } \forall f_i \in \mathcal{M} \ f_i(\mathbf{x}^1) \geq f_i(\mathbf{x}^2) \tag{1.3}$$

A solution $\mathbf{x}^1 \in X$ is *non-dominated* if

$$\nexists \mathbf{x}^2 \in X : \mathbf{x}^2 \succ \mathbf{x}^1 \tag{1.4}$$

The set of non-dominated solutions to the multi-objective problem (1.1) and (1.2) is referred to as the *Pareto-optimal set* $P = \{\mathbf{x} \in X | \nexists \mathbf{y} \in X : \mathbf{y} \succ \mathbf{x}\}$.

The *Pareto-optimal frontier*, the *efficient frontier* or, simply, the *frontier* Z is the corresponding set of M-dimensional *objective vectors* $\mathbf{z} = [f_1(\mathbf{x}), f_2(\mathbf{x}), \ldots, f_M(\mathbf{x})]$. That is,

$$Z = \{\mathbf{z} = [f_1(\mathbf{x}), \ldots, f_M(\mathbf{x})] \mid \mathbf{x} \in P\} \tag{1.5}$$

Objective vectors' components are referred to in subscripts:

$$\mathbf{z} = [z_1, z_2, \ldots, z_M] \tag{1.6}$$

Ideal and nadir objective vectors   The *ideal objective vector* is defined as the vector

$$\mathbf{z}^{\text{ideal}} = \max_{\mathbf{x} \in X}\{f_i(\mathbf{x})\} \quad \forall i \in \mathcal{M}. \tag{1.7}$$

Analogously, define the nadir solution as the vector

$$\mathbf{z}^{\text{nadir}} = \min_{\mathbf{x} \in X}\{f_i(\mathbf{x})\} \quad \forall i \in \mathcal{M}. \tag{1.8}$$

Sub-dimensions   Define the *sub-dimensional objective set* $\mathcal{L} \subset \mathcal{M}$ as a subset of the objective functions $f_i \in \mathcal{M}$. Call the cardinality of this set L. The *sub-dimensional objective vector* (specifically, the L-dimensional objective vector) for the solution $\mathbf{x}^i$ is the vector denoted $\mathbf{z}^i_{\mathcal{L}}$ whose components are $z^i_\ell = f_\ell(\mathbf{x}^i)$, $\forall \ell \in \mathcal{L}$. That is, they are the components of $\mathbf{z}^i$ that correspond to the objectives in $\mathcal{L}$.

Trade-offs   The *trade-off* between two objective vectors $\mathbf{z}^1$ and $\mathbf{z}^2$ is the vector of differences in their objective achievements:

$$\tau^{1,2} = [z_1^2 - z_1^1, z_2^2 - z_2^1, \ldots, z_M^2 - z_M^1] \tag{1.9}$$

Note that $\tau^{1,2} = -\tau^{2,1}$.

Given a sub-dimensional objective set $\mathcal{L}$, define the *sub-dimensional trade-off* $\tau_{\mathcal{L}}^{1,2}$ as the vector with components $\tau_\ell^{1,2}$, $\forall \ell \in \mathcal{L}$.

Relative objective achievements, relative objective vectors, and relative trade-offs   For an objective vector $\mathbf{z}$, its *relative achievement in objective i* is

$$\overline{z_i} = \frac{z_i - z_i^{\text{nadir}}}{z_i^{\text{ideal}} - z_i^{\text{nadir}}}, \tag{1.10}$$

and the corresponding *relative objective vector* is

$$\bar{\mathbf{z}} = [\overline{z_1}, \overline{z_2}, \ldots, \overline{z_M}]. \tag{1.11}$$

For two objective vectors $\mathbf{z}^1$ and $\mathbf{z}^2$, the corresponding *relative trade-off* is

$$\bar{\tau}^{1,2} = \left[\overline{z_1^2} - \overline{z_1^1}, \overline{z_2^2} - \overline{z_2^1}, \ldots, \overline{z_M^2} - \overline{z_M^1} \right] \tag{1.12}$$

Conflict, monotonicity, bundles and stacks   Objectives in an objective set $\mathcal{L}$ *do not conflict* if the objectives improve simultaneously: $\forall \mathbf{z}^1, \mathbf{z}^2 \in Z, i \in \mathcal{L}$

$$(z_i^1 \geq z_i^2) \Rightarrow (z_j^1 \geq z_j^2) \quad \forall j \in \mathcal{L}, j \neq i \tag{1.13}$$

If (1.13) does not hold, then the objectives conflict. Any pair of objectives $i, j \in \mathcal{M}$ such that equation (1.13) holds are said to *increase monotonically.* Conversely, if

$$(z_i^1 \geq z_i^2) \Rightarrow (z_j^1 \leq z_j^2) \quad \forall \mathbf{z}^1, \mathbf{z}^2 \in Z, j \neq i \tag{1.14}$$

holds, then the objectives are said to *decrease monotonically.* When the objectives represent goods or services, a set of objectives that conflict is defined as a *bundle* and a set of objectives that do not conflict is defined as a *stack.*

Equation (1.13) checks for monotonically increasing relationships among objectives. This means of detecting conflict among objectives in an objective set is functionally equivalent to that used by other studies, such as Brockhoff and Zitzler (2009) [10] and Purshouse and Fleming (2003) [59].

1.2.2   Measuring conflict

After determining that objectives conflict with one another, one may wish to determine the severity of the conflict. HYPERVOL HERE.

1.2.3   A new measure of conflict

Consider the frontiers in Figure 1.1. The conflict between maximization objectives i and j is greatest in Frontier C and least in Frontier A.
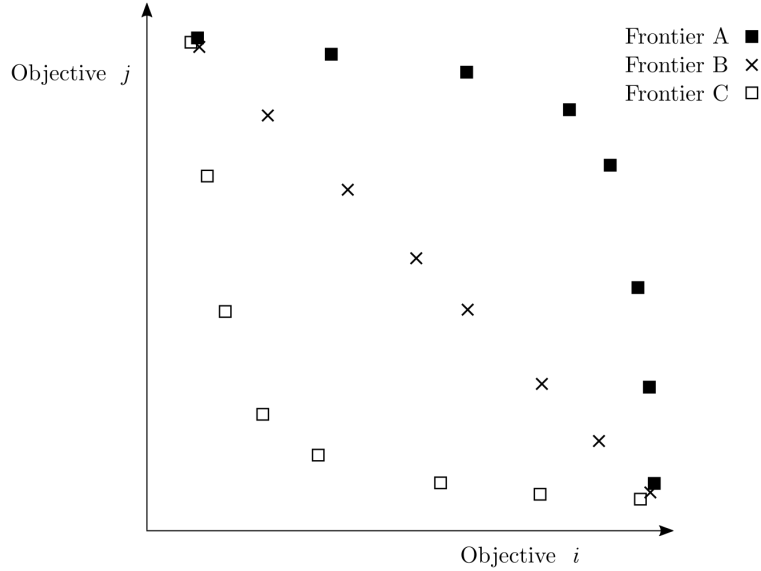

Figure 1.1: Varying conflict between objectives. The conflict between maximization objectives i and j increases from Frontier A to Frontier B to Frontier C.

Many authors have previously measured conflict between objectives [10][59][33], with most commonly used metrics deriving from measures of linear correlation (such as the Pear-

son correlation coefficient [22]) or rank correlation (such as Kendall's Tau [41] or Spearman's rho [43]). The intended use of these metrics is often the removal of redundant objectives from a many-objective optimization problem. In such cases, measures of monotonicity or correlation alone are adequate. However, the current metrics fall short of providing a robust quantification of conflict between a pair of objectives. Metrics for linear correlation are limited in their ability to capture the montonicity between objectives, which is the fundamental principle that determines if objectives conflict. Furthermore, both linear and rank correlation metrics fail to capture solutions' objective achievement. Thus, for a more nuanced understanding of the relationship between the objectives, a different metric is required.

Let $\mathbf{z}_{ij}$ be the sub-dimensional objective vector comprised of only the components corresponding to the ith and jth objectives $\mathbf{z}_{ij} = [z_i, z_j]$. I define the following measure of conflict between objectives i and j:

$$C_{ij} = \frac{(1 - \rho_{ij})\bar{d}_{ij}}{2d_{\mathrm{max},ij}} \tag{1.15}$$

where $\bar{d}_{ij}$ is the average sub-dimensional distance from objective vectors to the ideal solution:

$$\bar{d}_{ij} = \frac{1}{|Z|} \sum_{\mathbf{z} \in Z} ||\mathbf{z}_{ij}^{\mathrm{ideal}} - \mathbf{z}_{ij}|| \tag{1.16}$$

and

$$d_{\mathrm{max},ij} = ||\mathbf{z}_{ij}^{\mathrm{ideal}} - \mathbf{z}_{ij}^{\mathrm{nadir}}|| \tag{1.17}$$

and ρ_{ij} is Spearman's rank-correlation coefficient for the solutions' achievements in objectives i and j. Note that $C_{ij} \in [0, 1)$, taking smaller values when there is less conflict between objectives i and j and larger values when there is more.

The conflict metric proposed here (equation (1.15)) addresses two major issues:

1. **Indifference to non-conflicting relationships**. Per equation (1.13), when an objective i increases monotonically with another objective j the objectives do not conflict. Accordingly, C_{ij} should equal 0 in all such cases. This is true for the new metric, since for monotonically increasing objectives $\rho_{ij} = 1$, so $1 - \rho_{ij} = 0$.

2. **Consideration of objective achievement**. Recall Figure 1.1 and the intuitive notion that the conflict between objectives i and j is stronger in Frontier C than it is in Frontier B than it is in Frontier A. This notion is guided by the idea that the closer objective vectors are to the sub-dimensional ideal solution on average, the less the conflict between the objectives. That is, that greater simultaneous objective provision is indicative of less conflict. The proposed metric accounts for this, while correlation measures do not. In the extreme case of monotonically decreasing objectives, $\frac{(1-\rho_{ij})}{2} = 1$, so $C_{ij} = \frac{\bar{d}_{ij}}{d_{\max,ij}}$. See Figure 1.2 for an example.

	Proposed C_{ij}	Pearson ρ_{ij}	Spearman $\rho_{s,ij}$
Frontier A	0.4	-0.6	-1
Frontier B	0.6	-1	-1
Frontier C	0.8	-0.6	-1
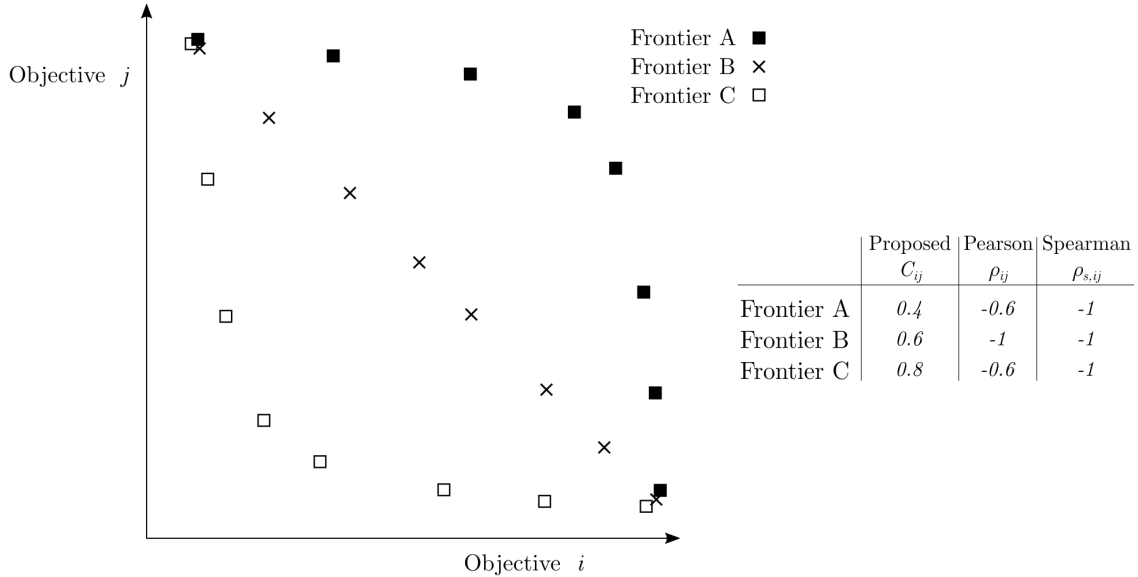
Figure 1.2: Comparing the proposed metric for conflict C_{ij} against the Pearson product-moment and the Spearman rank correlation coefficients (ρ_{ij} and $\rho_{s,ij}$, respectively). While the latter two are identical for frontiers A and C, the proposed metric is greater for frontier C than it is for A. This is because it accounts for the average relative distance to the sub-dimensional ideal objective vector.

1.2.4 Frontier-level conflict metrics

Above metric is good for 2d frontiers or for obj-pair comparisons within a frontier with M > 3. But for comparing entire frontiers when M > 3, we need dif metrics. We developed

an algorithm to compute this thing called hypervol. It's awesome (see appendix). Then we found out that it isn't new, actually. Then we found some other metrics. These are them. See the appendix (again).

1.2.5   Study system

To quantify the impacts of climate change on the relationships among and the joint provision of bundled forest ecosystem services, I employ multi-objective optimization on a study system in the Deschutes National Forest known as the Drink Planning Area. The Drink Area is a 7056 ha area on the east slopes of the Cascade Mountain Range (see Figure 1.3). Like many forests, the Drink is managed for the simultaneous provision of multiple ecosystem services. The ecosystem services were selected through a process involving stakeholder meetings and discussions regarding compatible ecosystem services. For the current work, a subset of the chosen ecosystem services was selected for study. While the USFS manages for many services simultaneously, many of the services are "stacked" rather than bundled, meaning that the ecosystem services are not in conflict. That is, maximizing the provision of one ecosystem service simultaneously maximizes another. Stacked ecosystem services need not all be studied with multi-objective optimization, since the selection and maximization of one ecosystem service entails the maximization of all in the stack. For that reason, we disregard non-conflicting ecosystem services and select a minimal bundle on which to employ multi-objective optimization. Those that do not conflict can be stacked post-optimization.

The minimal bundle selected for this case study is a set of three ecosystem services. The Forest Service seeks to ensure their sustained provision, and this may require an understanding of how these ecosystem services are impacted, jointly and independently, by climate change.

The first of these ecosystem services is the provision of habitat for the northern spotted owl (NSO) (*Strix occidentalis caurina*). The NSO is a common, if controversial, indicator species in Pacific Northwest forests. Because of the availability of dense old growth forest in the Drink, approximately 43% of the area serves as habitat for the NSO (see Figure 1.4). The

Figure 1.3: Overview of the study system, the Drink Planning Area (in purple), consisting of 7056 ha in the Deschutes National Forest.

USFS is required to protect this species as it is listed as threatened and therefore protected by the Endangered Species Act of 1973 [13].

The second ecosystem service the USFS seeks to provide is protection from high severity wildfire. This protection is achieved by way of silvicultural treatments applied to designated treatment areas (forest stands) across the Drink. The types of treatments assigned are defined in the appendix, §B. The efficacy of these treatments is measured by comparing the fire hazard rating of the stand before and after treatment. The fire hazard rating is described in more detail later and is summarized in Table 1.1. Implementing the silvicultural treatments to reduce the fire hazard rating of the Drink is critical not only because it protects the habitat of the NSO, but also because the Drink Area houses the municipal watershed
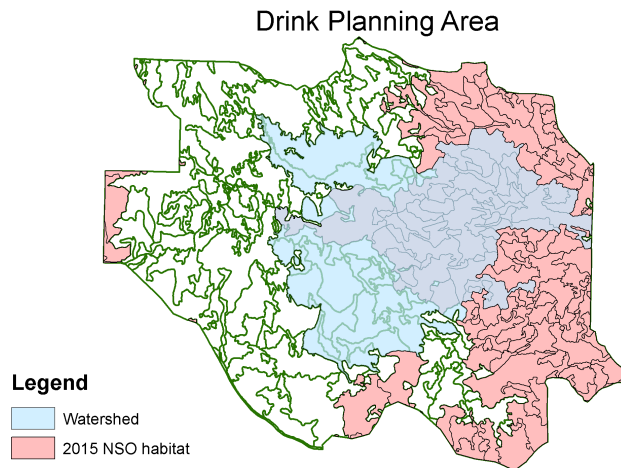
Figure 1.4: Location of the municipal watershed and the suitable NSO habitat in the Drink area at the beginning of the planning horizon (2015). Interior polygons are the 303 management units.

for the cities of Bend, OR and Sisters, OR (see Figure 1.4). Wildfires pose a threat to these cities' water supply, because wildfires can cause soil water repellency, surface runoff, and debris torrents [39] which would degrade the quality of the watershed. In addition, the Drink has never before undergone fuels treatments, which increases the expected severity of a fire should one occur.

Finally, the Forest Service seeks to provide a watershed with minimal sediment content. While the silvicultural treatments intend to provide long-term protection of the watershed, the implementation of the treatments has the potential to introduce short-term increases in sediment delivery [55]. This is expected to be especially true in the Drink Area, where local Forest Service staff have noted that the watershed is unusually susceptible to spikes in sediment delivery as a result of foot traffic and activities that occur within the watershed.

The changing climate will likely impact the provision of these ecosystem services and their relationships with one another. The extent of these changes will depend on the severity of the realized climate change. Thus, to understand the potential impacts, multiple climate change scenarios representing a range of severities must be considered. The following section

describes the climate scenarios considered in this case study.

1.2.6   Climate Scenarios Considered

In their assessments on the changing climate, the Intergovernmental Panel on Climate Change (IPCC) uses a scenario-based approach, considering many models of future climates from research groups around the world. They make no attempt to predict which of the future climates is most likely or to quantify the probability of realization of any one scenario. This same scenario-based approach is employed here in studying the potential impacts of climate change on trade-off relationships among bundled ecosystem services.

Here, the alternative future climates considered are climate scenarios from the first working group (WG1) of the IPCC's Fifth Assessment (AR5) [38]. Given the large number of potential future climates considered by the IPCC (see the list of experiments considered in AR5 [26]) combined with the computational complexity involved in the study of each one, I selected a subset of three future climate scenarios for this analysis. Hereafter the scenarios are referred to as "None", "Ensemble RCP 4.5", and "Ensemble RCP 8.5".

The first scenario, "None", is the assumption of no climate change. While the number of studies incorporating climate change is increasing, this is still the assumption used for many modern studies such as Schroder (2013) [64], from which this study is derived. Because it has served as the basis for many studies and assumes a static climate resembling today's, the "None" climate scenario serves as a control against which to compare the other two future climate scenarios.

As their names suggest, the second and third scenarios are ensembles. Each ensemble is an assembly of 17 global circulation models (GCMs) used in IPCC AR5. The selection of component GCMs in the ensembles was performed by the USFS's Climate-Forest Vegetation Simulator (FVS) [25] team. The list of the 17 scenarios included in the ensemble can be found in Crookston (2016) [16]. Each component GCM has a corresponding climate surface which contains a vector of 35 climate parameters at over 11,000 global locations for three time periods. The climate surfaces for the ensembles were created by averaging the values

of all component GCMs for each climate parameter and each time period for each location. The result is a climate surface that, while temporally sparse, is spatially robust. Such a configuration is well-suited for use in the Drink Area given the area's variance in elevation and slow vegetation growth.

The two ensembles are comprised of the same 17 GCMs, but the assumed representative concentration pathways (RCP) in the component GCMs differ. The RCP indicates the additional radiative forcing in W/m^2 above pre-industrial levels, with higher values of forcing indicative of more severe climate change. The GCMs in the Ensemble RCP 4.5 scenario assume 4.5 W/m^2 of additional radiative forcing, and the GCMs in the Ensemble RCP 8.5 scenario assume 8.5 W/m^2 of additional radiative forcing.

These three chosen scenarios represent a range of predicted climate change severity, from a $0°C$ warming by the year 2100 under the "None" scenario to a $2.6 - 4.8°C$ warming under RCP 8.5 [38]. Comparing the trade-off relationships among the ecosystem services under this range of climate change severities allows for the quantification of the impacts of climate.

1.2.7 The Multi-objective Optimization Model

In order to determine trade-off relationships among ecosystem services under each climate scenario, I employ multi-objective spatial optimization. This section describes the multi-objective zero-one mathematical program to optimize the joint provision of ecosystem services in the Drink Area. The model operates over an 80-year planning horizon (2015-2095) in which it assigns silvicultural treatments to forest stands that will be performed in the first or second 20 year period (2015-2035 or 2035-2055). Determining which treatment type to apply to a stand was done *a priori* and is entirely dependent on silvicultural characteristics; the rules governing this assignment of treatment type can be found in the appendix, §B.

The model minimizes the fire hazard rating of the Drink at the end of the 80-year planning horizon, maximizes the area of NSO habitat at the end of each planning period, and minimizes the short-term spikes in sediment delivery resulting from the application of silvicultural treatments.
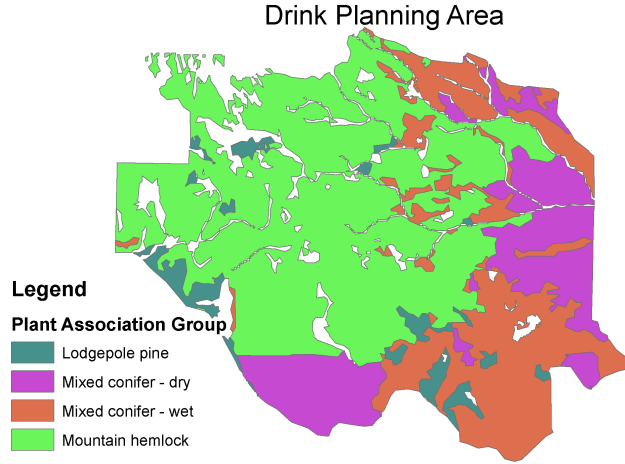
Figure 1.5: Plant association groups in the Drink Planning Area that were selected for potential treatments. Other plant association groups exist in the area but were not considered for treatment.

Treatments are assumed to be performed at the midpoint year in the treatment period, years 2025 and 2045 for the first and second periods, respectively. A schematic of the planning horizon including the time of these events is shown in Figure 1.6.

Notation

The following notation is used throughout the model:

Parameters

- $i \in I$: the set of all 303 forest stands comprising the Drink area

- $r \in R$: the set of treatment schedule prescriptions:

$$
r = \begin{cases}
1 & \text{treatment applied in the first period (2015-2035)} \\
2 & \text{treatment applied in the second period (2035-2055)} \\
3 & \text{treatment applied in both periods} \\
0 & \text{no treatment applied in either period}
\end{cases}
$$

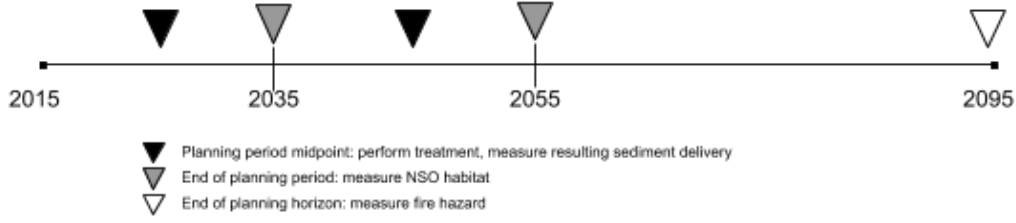Figure 1.6: The planning horizon used in the analysis spans the 80 year period from 2015 to 2095. Treatments may be performed in the first period, the second period, both, or neither. Treatments are assumed to be performed at the mid-point years of each period (black triangles). Sediment delivery is measured on treatment years. Stands' suitability for NSO habitat is measured at the end of the planning periods (gray triangles), and stands' fire hazard ratings are measured at the end of the planning horizon (white triangle).

- $F_{i,r}$: the area-weighted fire hazard rating of stand i at the end of the planning horizon if prescribed to treatment schedule r

- $I_{\omega,t}$: the set of stands that can qualify as NSO habitat at the end of planning period t

- a_i: the area of stand i

- e: the discount factor applied to NSO habitat that is less than 200 ha in size

- $j \in R_{i,t}$: the set of treatment schedules such that stand i qualifies as NSO habitat in planning period t

- $s_{i,t}$: the contribution in tons of sediment delivered from performing fuel treatments on stand i in planning period t

- $c \in C$: the set of all clusters of stands whose combined area exceeds 200 hectares

- $i \in D_c$: the set of all stands that comprise cluster c

- $c \in C_i$: the set of all clusters that contain stand i

- A: the maximum area in hectares that may be treated in either planning period

- ℓ, u: the lower and upper bounds, respectively, on the relative fluctuation in the area treated in periods 1 and 2

Decision Variables

$$x_{i,r} = \begin{cases} 1 & \text{if stand } i \text{ is prescribed to treatment schedule } r \\ 0 & \text{otherwise} \end{cases}$$

Indicator Variables

- $q_{c,t} = 1$ if all stands in cluster c qualify as NSO habitat in planning period t and $q_{c,t} = 0$ otherwise

- $p_{i,t} = 1$ if in planning period t stand i is part of a cluster c such that $q_{c,t} = 1$; $p_{i,t} = 0$ otherwise

Accounting Variables

- S_t: the contribution in tons of sediment delivered from performing fuel treatments in planning period t

- O_t: the amount of NSO habitat in hectares at the end of planning period t

- H_t: the area in hectares treated in planning period t

Parameterization

The model was parameterized as follows:

- $F_{i,r}$: the metric for fire hazard rating used in this analysis originated in the work by Schroder *et al.* [64]. This metric was developed for the Drink area. It uses fire

characteristics from Anderson's fuel models [4] to assign a fire hazard rating. I expanded the rating system to include fuel models not present in Schroder *et al.* See Table 1.1.

The stands' fuels and vegetation characteristics to determine the fire hazard rating were generated using the US Forest Service's Climate-Forest Vegetation Simulator (FVS). Input vegetation data to Climate-FVS came from the 2012 GNN structure map (`http://lemma.forestry.oregonstate.edu/data/structure-maps`) from Oregon State University's Landscape Ecology, Modeling, Mapping & Analysis (LEMMA) group. Plots from the LEMMA database were mapped to the stands in the Drink area in order to produce tree and stand lists. These lists were used with Climate-FVS to simulate the stands' vegetation and fuels characteristics forward for the duration of the planning horizon under each climate scenario. Input climate data for Climate-FVS was obtained through the Climate-FVS climate data server [17].

- $I_{\omega,t}$: the set of stands that qualify as NSO habitat at the end of a planning period t are those that meet the following three criteria, as specified by the USFS:

  1. elevation less than 1830 m

  2. the presence of trees with DBH no less than 76 cm

  3. canopy closure of at least 60%

  The elevation requirement was checked using a digital elevation model from the US Department of Agriculture's GeoSpatial Data Gateway; canopy closure and large tree requirements were determined using the simulated vegetation characteristics output from Climate-FVS.

  To account for the NSO's large habitat requirements, stands must also be members of a cluster exceeding 200 ha in size, the entirety of which meets the aforementioned NSO habitat criteria. Stands not part of such a cluster have their contributions to owl habitat discounted by a factor of e.

- e: the discount factor for sub-200 ha NSO habitat was set to $e = 0.5$ following the convention used in Schroder *et al.* [64].

- $j \in R_{i,t}$: each stand-treatment schedule combination is evaluated at the end of each planning period to determine its suitability as NSO habitat. Treatment schedules for which stand i meets the NSO habitat criteria at the end of treatment period t become members of the set $R_{i,t}$.

- $s_{i,t}$: the contributions of sediment delivery from treatment of stand i in period t were determined using the Watershed Erosion Prediction Project (WEPP) online GIS tool [31]. This tool takes as input soil textures, treatment types, duration of simulation, and custom climate data. Soil texture data for the Drink area was obtained from the USDA's Soil Survey Geographic (SSURGO) database, treatment types are those specified in §B, and the years of simulation correspond to the treatment years in the model's planning horizon (2015-2095). The custom climate data are those described above for use with Climate-FVS, obtained through the Climate-FVS data server.

- C,D_c,C_i: the formulation of clusters was performed *a priori* according to the algorithm used in Rebain and McDill (2003) [60]. The enumerated clusters can then be used to immediately determine cluster members D_c and stand-owning clusters C_i.

- A: the maximum area that may be treated in either planning period was defined to be 6000 acres, or approximately 2428 ha

- ℓ, u: the relative fluctuation in the area treated in periods 1 and 2 was defined to be 20%. That is, the lower bound $\ell = 0.8$, and the upper bound $u = 1.2$.

Fuel Model	Fire Hazard Rating	Group	Flame length (m)	Rate of spread (m/hr)	Total fuel load (tons/ha)
4*	**5**	Shrub	5.79	1508.76	32.12
5	**4**	Shrub	1.22	362.10	8.65
8	**1**	Timber	0.30	32.19	12.36
9*	**2**	Timber	0.79	150.88	8.65
10	**2**	Timber	1.46	158.92	29.65
11*	**2**	Logging Slash	1.07	120.7	28.42
12	**4**	Logging Slash	2.44	261.52	85.50
13	**5**	Logging Slash	3.20	271.58	143.57

Table 1.1: Fire hazard rating system used here, originally employed by Schroder *et al.* [64]. Asterisks (*) denote fuel models not present in Schroder *et al.*
The fuel model column refers to the Anderson fuel model ratings [4].

Formulation

The formulation of the model is as follows:

Minimize

$$\sum_{i \in I} \sum_{r \in R} F_{i,r} x_{i,r} \tag{1.18}$$

$$\max\{S_1, S_2\} \tag{1.19}$$

Maximize

$$\min\{O_1, O_2\} \tag{1.20}$$

Subject to:

$$\sum_{i\in I_{\omega,t}}\left(a_i p_{i,t} + ea_i\left(\sum_{j\in R_{i,t}} x_{i,j} - p_{i,t}\right)\right) = O_t \qquad \forall t \in \{1,2\} \tag{1.21}$$

$$\sum_{i\in I}\sum_{r\in 1,3} s_{i,1}x_{i,r} = S_1 \tag{1.22}$$

$$\sum_{i\in I}\sum_{r\in 2,3} s_{i,2}x_{i,r} = S_2 \tag{1.23}$$

$$\sum_{i\in D_c}\sum_{j\in R_{i,t}} x_{i,j} - |c|q_{c,t} \geq 0 \qquad \forall t \in \{1,2\}, c \in C \tag{1.24}$$

$$\sum_{c\in C_i} q_{c,t} - p_{i,t} \geq 0 \qquad \forall t \in \{1,2\}, i \in I_{\omega,t} \tag{1.25}$$

$$\sum_{r\in R} x_{i,r} = 1 \qquad \forall i \in I \tag{1.26}$$

$$\sum_{i\in I}\sum_{r\in 1,3} a_i x_{i,r} = H_1 \tag{1.27}$$

$$\sum_{i\in I}\sum_{r\in 2,3} a_i x_{i,r} = H_2 \tag{1.28}$$

$$H_t \leq A \qquad \forall t \in \{1,2\} \tag{1.29}$$

$$\ell H_1 - H_2 \leq 0 \tag{1.30}$$

$$-uH_1 + H_2 \leq 0 \tag{1.31}$$

$$x_{i,r}, p_i, q_c \in \{0,1\} \quad \forall i \in I, r \in R, c \in C \tag{1.32}$$

Equations (1.18)-(1.20) are the objective functions: equation (1.18) minimizes the cumulative fire hazard rating of the Drink area at the end of the 80-year planning horizon, equation (1.19) minimizes the maximum peak in sediment delivery for the two planning periods, and equation (1.20) maximizes the minimum NSO habitat available at the end of the planning periods. Equation set (1.21) defines the amount of NSO habitat available at the end of the planning horizons. Note that if stand i does not belong to a cluster of NSO habitat exceeding 200 hectares, then its area contribution to total NSO habitat is discounted by a factor of e. Equations (1.22) and (1.23) define the sediment delivered in planning periods one and two,

respectively.

Inequality set (1.24) controls the value of the cluster variables $q_{c,t}$ indicating clusters meeting NSO habitat criteria in each of the planning periods. Inequality set (1.25) controls the value of the $p_{i,t}$ variables indicating stands' inclusion in NSO habitat clusters.

The set of equalities (1.26) enforces the logical constraint that each stand must be prescribed to exactly one treatment schedule. Equations (1.27) and (1.28) are accounting constraints for the total area treated in each planning period, and inequalities (1.29) ensure that this area does not exceed the predefined per-period maximum. Inequalities (1.30) and (1.31) bound the fluctuation in treated area between the planning periods. Finally, constraint (1.32) defines the decision and indicator variables as binary.

1.2.8 Model Solution and Comparing Efficient Frontiers

I developed an implementation of Tóth's Alpha-Delta algorithm [70] to solve the models utilizing the IBM ILOG CPLEX optimization engine. For a problem with N objectives, the Alpha-Delta algorithm finds the optimal set of solutions by iteratively slicing the N-dimensional objective space with a tilted $N - 1$ dimensional plane. The algorithm was implemented using an alpha parameter of $\alpha = .01$ and delta parameters of $\delta_{Hab} = 1$ ha and $\delta_{Sed} = 2$ tons for the NSO habitat and sediment delivery objectives, respectively.

The solution to a bounded and non-degenerate multi-objective optimization problem with N objectives is a set of objective vectors (also called "solutions") $\mathbf{z} \in Z$ where $\mathbf{z} = [z^1, \ldots, z^N]$. The set of solutions Z is referred to as the Pareto-optimal frontier or efficient frontier or, simply, frontier. The solutions comprising an efficient frontier have the special relationship such that no component of a solution $\mathbf{z}^i$ can be improved upon without one of the other components $\mathbf{z}^j$ $(j \neq i)$ degrading. This quality is known as Pareto efficiency. For example, this relationship in the current problem means that further reducing the value of fire hazard in a solution would result in either additional sediment delivery, a reduction of NSO habitat, or both.

Thus the efficient frontier provides information on the trade-off relationship that exists

between ecosystem services. Parameterizing and solving the above model for each of the climate scenarios generates three frontiers: Z_{None}, $Z_{4.5}$, and $Z_{8.5}$ for the None, Ensemble RCP 4.5, and Ensemble RCP 8.5 scenarios, respectively. Since climate data alone differentiates the models and their resulting frontiers, comparing the frontiers reveals the impacts of climate on the trade-off relationships among the ecosystem services. However, no standardized procedure exists to compare frontiers.

One applicable metric to compare frontiers is the volume of the N-dimensional objective space bounded by the frontier, known as the hypervolume indicator. Together with Sándor Tóth, I devised an algorithm to compute the value of the hypervolume indicator any general N-dimensional frontier. The algorithm proceeds by sorting the solutions according to one objective, then iteratively adding them to the frontier, each time computing the additional volume enclosed by the solution. Details of the algorithm may be found in the appendix, §A.

We developed this algorithm independently and later discovered that researchers in the field of Evolutionary Multi-objective Optimization (EMO) have developed similar algorithms to compute the hypervolume indicator. In the present study, the hypervolume indicator is used as a measure of conflict among ecosystem services. Comparing hypervolume indicators across frontiers offers a quantification of the impact of climate change on trade-off relationships among ecosystem services. In EMO, the hypervolume indicator is used to assess the performance of stochastic multi-objective optimization algorithms. Hence, while the metric is the same, the algorithm to compute it and its application are entirely unique in this study.

Upon realization of the use of the hypervolume indicator in EMO, I discovered additional frontier comparison metrics used in this field and have adopted them for use here. These include the following indicators: the additive binary epsilon, binary hypervolume, unary distance, additive unary epsilon, and unary spacing. Information on these indicators can be found in the appendix, §C.1.

In addition to frontier-level comparisons that measure conflict between all ecosystem services simultaneously, it is also worthwhile to consider how climate change may impact

the relationship between two specific ecosystem services within the frontier. Here, I use two methods to determine this: 1) the hypervolume indicator of the nondominated frontier points in a 2D projection, and 2) the Pearson correlation coefficient between objectives. Details on these methods may be found in the appendix, §C.2.

1.3 Results and Discussion

DRAFT

The frontiers for each climate scenario can be found in Figure . . .

1.4 Conclusion

DRAFT

I find that climate change has positive impacts on the tradeoff structure between managed ecosystem services in the Drink Area . . .

BIBLIOGRAPHY

[1] 36 CFR 219.1. National forest system land management planning, 2012.

[2] Fouad Ben Abdelaziz. Solution approaches for the multiobjective stochastic programming. *European Journal of Operational Research*, 216(1):1–16, 2012.

[3] Frank A Albini. Estimating wildfire behavior and effects. 1976.

[4] Hal E Anderson. Aids to determining fuel models for estimating fire behavior. *The Bark Beetles, Fuels, and Fire Bibliography*, page 143, 1982.

[5] Millennium Ecosystem Assessment et al. *Ecosystems and human well-being*, volume 5. Island press Washington, DC:, 2005.

[6] Brad Bass, Guohe Huang, and Joe Russo. Incorporating climate change into risk assessment using grey mathematical programming. *Journal of Environmental Management*, 49(1):107 – 123, 1997.

[7] Gordon B Bonan. Forests and climate change: forcings, feedbacks, and the climate benefits of forests. *Science*, 320(5882):1444–1449, 2008.

[8] Jose G Borges, Jordi Garcia-Gonzalo, Vladimir Bushenkov, Marc E McDill, Susete Marques, and Manuela M Oliveira. Addressing multicriteria forest management with pareto frontier methods: An application in portugal. *Forest Science*, 60(1):63–72, 2014.

[9] Dimo Brockhoff and Eckart Zitzler. Are all objectives necessary? on dimensionality reduction in evolutionary multiobjective optimization. In *Parallel Problem Solving from Nature-PPSN IX*, pages 533–542. Springer, 2006.

[10] Dimo Brockhoff and Eckart Zitzler. Objective reduction in evolutionary multiobjective optimization: Theory and applications. *Evolutionary Computation*, 17(2):135–166, 2009.

[11] Brett A. Bryan and Neville D. Crossman. Systematic regional planning for multiple objective natural resource management. *Journal of Environmental Management*, 88(4):1175 – 1189, 2008.

[12] Kai MA Chan, M Rebecca Shaw, David R Cameron, Emma C Underwood, and Gretchen C Daily. Conservation planning for ecosystem services. *PLoS biology*, 4(11):e379, 2006.

[13] US Congress. Endangered species act. *Washington DC*, 1973.

[14] Ira R. Cooke, Simon A. Queenborough, Elizabeth H. A. Mattison, Alison P. Bailey, Daniel L. Sandars, A. R. Graves, J. Morris, Philip W. Atkinson, Paul Trawick, Robert P. Freckleton, Andrew R. Watkinson, and William J. Sutherland. Integrating socio-economics and ecology: a taxonomy of quantitative methods and a review of their use in agro-ecology. *Journal of Applied Ecology*, 46(2):269–277, 2009.

[15] Steven P Courtney and Andrew B Carey. *Scientific evaluation of the status of the Northern Spotted Owl*. Sustainable Ecosystems Institute Portland, OR, 2004.

[16] Nicholas Crookston. Details of data and methods used for calculating future climate estimates, 2016.

[17] Nicholas Crookston. Get climate-fvs ready data, 2016.

[18] Nicholas L Crookston. Climate-fvs version 2: Content, users guide, applications, and behavior. 2014.

[19] Piotr Czyzżak and Adrezej Jaszkiewicz. Pareto simulated annealingâĂŤa metaheuristic technique for multiple-objective combinatorial optimization. *Journal of Multi-Criteria Decision Analysis*, 7(1):34–47, 1998.

[20] Gretchen C Daily, Susan Alexander, Paul R Ehrlich, Larry Goulder, Jane Lubchenco, Pamela A Matson, Harold A Mooney, Sandra Postel, Stephen H Schneider, David Tilman, et al. *Ecosystem services: benefits supplied to human societies by natural ecosystems*, volume 2. Ecological Society of America Washington (DC), 1997.

[21] Kalyanmoy Deb. *Multi-objective optimization using evolutionary algorithms*, volume 16. John Wiley & Sons, 2001.

[22] Kalyanmoy Deb and D Saxena. Searching for pareto-optimal solutions through dimensionality reduction for certain large-dimensional multi-objective optimization problems. In *Proceedings of the World Congress on Computational Intelligence (WCCI-2006)*, pages 3352–3360, 2006.

[23] Kalyanmoy Deb and Dhish Kumar Saxena. On finding pareto-optimal solutions through dimensionality reduction for certain large-dimensional multi-objective optimization problems. *Kangal report*, 2005011, 2005.

[24] Luis Diaz-Balteiro and Carlos Romero. Making forestry decisions with multiple criteria: a review and an assessment. *Forest Ecology and Management*, 255(8):3222–3241, 2008.

[25] Gary E Dixon et al. Essential fvs: A userâĂŹs guide to the forest vegetation simulator. *Fort Collins, CO: USDA-Forest Service, Forest Management Service Center*, 2002.

[26] German Climate Computing Centre (DKRZ). IPCC working group i AR5 snapshot.

[27] Oregon Fish and Wildlife Office. Species fact sheet: Northern spotted owl. `http://www.fws.gov/oregonfwo/Species/Data/NorthernSpottedOwl/default.asp`. Accessed: 2015-02-06.

[28] US Fish, Wildlife Service, et al. Revised recovery plan for the northern spotted owl (strix occidentalis caurina). *USDI Fish and Wildlife Service, Portland, OR USA*, 2011.

[29] Forestières Internationaler Verband Forstlicher Forschungsanstalten. Adaptation of forests and people to climate change. 2009.

[30] Eclipse Foundation. Eclipse, 2014.

[31] James R Frankenberger, Shuhui Dun, Dennis C Flanagan, Joan Q Wu, and William J Elliot. Development of a gis interface for WEPP model application to great lakes forested watersheds. In *International Symposium on Erosion and Landscape Evolution (ISELE), 18-21 September 2011, Anchorage, Alaska*, page 139. American Society of Agricultural and Biological Engineers, 2011.

[32] William L Gaines, Richy J Harrod, James Dickinson, Andrea L Lyons, and Karl Halupka. Integration of northern spotted owl habitat and fuels treatments in the eastern cascades, washington, usa. *Forest Ecology and Management*, 260(11):2045–2052, 2010.

[33] Tomas Gal and Heiner Leberling. Redundant objective functions in linear vector maximum problems and their determination. *European Journal of Operational Research*, 1(3):176–184, 1977.

[34] J Garcia-Gonzalo, JG Borges, JHN Palma, and A Zubizarreta-Gerendiain. A decision support system for management planning of eucalyptus plantations facing climate change. *Annals of Forest Science*, 71(2):187–199, 2014.

[35] Jaime R. Goode, Charles H. Luce, and John M. Buffington. Enhanced sediment delivery in a changing climate in semi-arid mountain basins: Implications for water resource management and aquatic habitat in the northern rocky mountains. *Geomorphology*, 139âĂŞ140(0):1 – 15, 2012.

[36] Lee E Harding and Emily McCullum. Ecosystem response to climate change in british columbia and yukon: threats and opportunities for biodiversity. *Responding to global climate change in British Columbia and Yukon*, 1:9–1, 1997.

[37] Grant Hauer, Steve Cumming, Fiona Schmiegelow, Wiktor Adamowicz, Marian Weber, and Robert Jagodzinski. Tradeoffs between forestry resource and conservation values under alternate policy regimes: A spatial analysis of the western canadian boreal plains. *Ecological Modelling*, 221(21):2590 – 2603, 2010.

[38] IPCC Working Group I. *Climate Change 2013-The Physical Science Basis: Summary for Policymakers*. Intergovernmental Panel on Climate Change, 2013.

[39] George G Ice, Daniel G Neary, and Paul W Adams. Effects of wildfire on soils and watershed processes. *Journal of Forestry*, 102(6):16–20, 2004.

[40] Louis R Iverson and Anantha M Prasad. Predicting abundance of 80 tree species following climate change in the eastern united states. *Ecological Monographs*, 68(4):465–485, 1998.

[41] Evangelos Kanoulas and Javed A Aslam. Empirical justification of the gain and discount function for ndcg. In *Proceedings of the 18th ACM conference on Information and knowledge management*, pages 611–620. ACM, 2009.

[42] Amit Kanudia and Richard Loulou. Robust responses to climate change via stochastic markal: The case of quÃľbec. *European Journal of Operational Research*, 106(1):15 – 30, 1998.

[43] Prasad Karande and Shankar Chakraborty. Application of multi-objective optimization on the basis of ratio analysis (moora) method for materials selection. *Materials & Design*, 37:317–324, 2012.

[44] Vineet Khare, Xin Yao, and Kalyanmoy Deb. Performance scaling of multi-objective evolutionary algorithms. In *Evolutionary Multi-Criterion Optimization*, pages 376–390. Springer, 2003.

[45] Joshua Knowles and David Corne. On metrics for comparing nondominated sets. In *Evolutionary Computation, 2002. CEC'02. Proceedings of the 2002 Congress on*, volume 1, pages 711–716. IEEE, 2002.

[46] Danny C Lee and Larry L Irwin. Assessing risks to spotted owls from forest thinning in fire-adapted forests of the western united states. *Forest Ecology and Management*, 211(1):191–209, 2005.

[47] Marcus Linder. Developing adaptive forest management strategies to cope with climate change. *Tree Physiology*, 20(5-6):299–307, 2000.

[48] Alexander V Lotov, Vladimir A Bushenkov, and Georgy K Kamenev. *Interactive decision maps: Approximation and visualization of Pareto frontier*, volume 89. Springer, 2004.

[49] Alexander V Lotov and Kaisa Miettinen. Visualizing the pareto frontier. In *Multiobjective optimization*, pages 213–243. Springer, 2008.

[50] B Luo, I Maqsood, YY Yin, GH Huang, and SJ Cohen. Adaption to climate change through water trading under uncertainty- an inexact two-stage nonlinear programming approach. *Journal of Environmental Informatics*, 2(2):58–68, 2003.

[51] Shunsuke Managi. Evaluation and policy analysis of japanese forestry. In *2005 Annual meeting, July 24-27, Providence, RI*, number 19358. American Agricultural Economics Association (New Name 2008: Agricultural and Applied Economics Association), 2005.

[52] Donald McKenzie, Ze'ev Gedalof, David L Peterson, and Philip Mote. Climatic change, wildfire, and conservation. *Conservation Biology*, 18(4):890–902, 2004.

[53] Robin Naidoo, Andrew Balmford, Robert Costanza, Brendan Fisher, Rhys E Green, B Lehner, TR Malcolm, and Taylor H Ricketts. Global mapping of ecosystem services and conservation priorities. *Proceedings of the National Academy of Sciences*, 105(28):9495–9500, 2008.

[54] Craig R. Nitschke and John L. Innes. Integrating climate change into forest management in south-central british columbia: An assessment of landscape vulnerability and development of a climate-smart framework. 2008.

[55] Jay OâĂŹLaughlin. Conceptual model for comparative ecological risk assessment of wildfire effects on fish, with and without hazardous fuel treatment. *Forest Ecology and Management*, 211(1):59–72, 2005.

[56] Intergovernmental Panel on Climate Change. Definition of terms used within the DDC pages. `http://www.ipcc-data.org/guidelines/pages/definitions.html`, 2013.

[57] Intergovernmental Panel on Climate Change. Scenario Process for AR5. `http://sedac.ipcc-data.org/ddc/ar5\_scenario\_process/scenario\_background.html`, 2014.

[58] M. Pasalodos-Tato, A. MÃďkinen, J. Garcia-Gonzalo, J.G. Borges, T. LÃďmÃěs, and L.O. Eriksson. Review. assessing uncertainty and risk in forest planning and decision support systems: review of classical methods and introduction of new approaches. *Forest Systems*, 22(2), 2013.

[59] Robin C Purshouse and Peter J Fleming. Conflict, harmony, and independence: Relationships in evolutionary multi-criterion optimisation. In *International Conference on Evolutionary Multi-Criterion Optimization*, pages 16–30. Springer, 2003.

[60] Stephanie Rebain and Marc E McDill. A mixed-integer formulation of the minimum patch size problem. *Forest Science*, 49(4):608–618, 2003.

[61] Lester Henry Reineke. Perfecting a stand-density index for even-aged forests. 1933.

[62] Elizabeth Reinhardt and Nicholas L Crookston. The fire and fuels extension to the forest vegetation simulator. 2003.

[63] Jason R Schott. Fault tolerant design using single and multicriteria genetic algorithm optimization. Technical report, DTIC Document, 1995.

[64] Svetlana A (Kushch) Schroder, Sándor F Tóth, Robert L Deal, and Ettl Gregory J. Multi-objective optimization to evaluate tradeoffs among forest ecosystem services following fire hazard reduction in the Deschutes National Forest, USA. *Ecosystem Services*, Special Issue "Integrated Valuation of Ecosystem Services: Challenges and Solutions", accepted.

[65] Svetlana Kushch Schroder. *Optimizing forest management in consideration of environmental regulations, economic constraints, and ecosystem services*. PhD thesis, 2013.

[66] Rupert Seidl, Werner Rammer, Dietmar Jäger, and Manfred J Lexer. Impact of bark beetle (< i> ips typographus</i> l.) disturbance on timber production and carbon sequestration in different management strategies under climate change. *Forest Ecology and Management*, 256(3):209–220, 2008.

[67] Daniel Simberloff. Flagships, umbrellas, and keystones: is single-species management passé in the landscape era? *Biological conservation*, 83(3):247–257, 1998.

[68] Soil Survey Staff. Soil survey geographic (ssurgo) database.

[69] Chris D Thomas, Alison Cameron, Rhys E Green, Michel Bakkenes, Linda J Beaumont, Yvonne C Collingham, Barend FN Erasmus, Marinez Ferreira De Siqueira, Alan Grainger, Lee Hannah, et al. Extinction risk from climate change. *Nature*, 427(6970):145–148, 2004.

[70] Sándor Tóth. *Modeling Timber and Non-timber Trade-offs in Spatially-Explicit Forest Planning.* PhD thesis.

[71] Sándor Tóth and Marc McDill. Finding efficient harvest schedules under three conflicting objectives. 2009.

[72] Sándor Tóth, Marc McDill, and Stephanie Rebain. Finding the efficient frontier of a bi-criteria, spatially explicit, harvest scheduling problem. 2006.

[73] Sándor F Tóth and Marc E McDill. Finding efficient harvest schedules under three conflicting objectives. *Forest Science*, 55(2):117–131, 2009.

[74] Fernando Badilla Veliz, Jean-Paul Watson, Andres Weintraub, Roger J-B Wets, and David L Woodruff. Stochastic optimization models in forest planning: a progressive hedging solution approach. *Annals of Operations Research*, pages 1–16, 2014.

[75] James M Vose, David Lawrence Peterson, Toral Patel-Weynand, et al. *Effects of climatic variability and change on forest ecosystems: a comprehensive science synthesis for the US forest sector.* US Department of Agriculture, Forest Service, Pacific Northwest Research Station Portland, OR, 2012.

[76] Andy White and Alejandra Martin. Who owns the worldâĂŹs forests. *Forest Trends, Washington, DC*, 2002.

[77] Steven M Wondzell and John G King. Postfire erosional processes in the pacific north-west and rocky mountain regions. *Forest Ecology and Management*, 178(1):75–87, 2003.

[78] Rasoul Yousefpour, Jette Bredahl Jacobsen, Bo Jellesmark Thorsen, Henrik Meilby, Marc Hanewinkel, and Karoline Oehler. A review of decision-making approaches to handle uncertainty and risk in adaptive forest management under climate change. *Annals of forest science*, 69(1):1–15, 2012.

[79] Eckart Zitzler. *Evolutionary algorithms for multiobjective optimization: Methods and applications*, volume 63. Citeseer, 1999.

[80] Eckart Zitzler, Lothar Thiele, Marco Laumanns, Carlos M Fonseca, and Viviane Grunert Da Fonseca. Performance assessment of multiobjective optimizers: an analysis and review. *Evolutionary Computation, IEEE Transactions on*, 7(2):117–132, 2003.

Appendix A

COMPUTING A FRONTIER'S HYPERVOLUME INDICATOR

Given a set of Pareto optimal solutions $\mathcal{P}$ to a multi-objective mathematical programming model with a set of objectives O of cardinality $N := |O|$, this algorithm computes the volume V of the objective space bounded by the Pareto frontier defined by the solutions $x \in \mathcal{P}$. The objectives are assumed to be normalized so that the objective space is the N-dimensional unit hypercube with the origin and the point $\vec{\mathbf{1}}$ defining the nadir objective vector and the ideal objective vector, respectively. That is, all objectives are assumed to be maximized with bounds $[0, 1]$.

The algorithm projects the objective space into $N - 1$ dimensions by eliminating the dimension associated with an (arbitrarily-chosen) objective $p \in O$. The set of objectives is $\overline{O} := O \backslash \{p\}$. It is assumed that $x \in \mathcal{P}$ are sorted in descending order according to p. The algorithm proceeds by sequentially adding solutions to the $(N - 1)$-dimensional space, and calculating the contribution to the frontier volume as a product of the volume contribution in $N - 1$ dimensions and its achievement in objective p.

Let $\overline{V_x}$ be the $(N - 1)$-dimensional volume contribution of solution x and x_p be the achievement of solution x in objective p. Further, let F be the set of non-dominated solutions in $N - 1$ dimensions. I compute the N-dimensional volume of the frontier V as follows.

Figure A.1: Algorithm to compute the unary hypervolume indicator of a Pareto frontier.

1: $V \leftarrow 0$

2: $\overline{V} \leftarrow 0$

3: $F \leftarrow \emptyset$

4: **for all** $x \in \mathcal{P}$ **do**

5:     $\overline{V}_x \leftarrow \prod_{o \in \overline{O}} x_o - \overline{V}$

6:     **for all** $f \in F$ **do**

7:         **if** $f_o < x_o \forall o \in \overline{O}$ **then**

8:             $F \leftarrow F \backslash \{f\}$

9:         **end if**

10:     **end for**

11:     **for all** $o \in \overline{O}$ **do**

12:         $F_{x,o} := \{ f \in F : f_o > x_o \}$

13:         Sort $f \in F_{x,o}$ in ascending order by their oth component, f_o

14:         $v_i \leftarrow x_o$

15:         **for all** $f \in F_{x,o}$ **do**

16:             $v_t \leftarrow f_o$

17:             $\delta_o := v_t - v_i$

18:             $\overline{V}_x \leftarrow \overline{V}_x + \delta_o \prod_{\sigma \in \overline{O} \backslash \{o\}} f_\sigma$

19:             $v_i \leftarrow v_t$

20:         **end for**

21:     **end for**

22:     $F \leftarrow F \cup \{x\}$

23:     $\overline{V} \leftarrow \overline{V} + \overline{V}_x$

24:     $V \leftarrow V + x_p \overline{V}_x$

25: **end for**

Appendix B

TREATMENT SPECIFICATIONS FOR THE DRINK AREA

Vegetation conditions were assessed at the midpoint of each planning period. If a set of conditions as listed in Table B.1 were met, then the corresponding treatment was applied. Otherwise, no action was taken. Table adapted from Schroder [64].

Table B.1: Rules governing treatment assignments.

SDI[1]	CBD[2]	TPH$_{<18}$[3]	Fuel model[4]	BA$_{\text{MHD+WF},>46}$[5]	Treatment
Lodgepole pine (LPD) plant association					
< 87	N/A	N/A	N/A	N/A	Prescribed burn
≥ 87	> 0.037	> 49	≥ 10	N/A	Thin, pileburn slash and fuels[6]
			< 10	N/A	Thin, pileburn slash
Mixed conifer wet (MCW) or mountain hemlock (MHD) plant associations					
< 87	N/A	N/A	N/A	N/A	Prescribed burn

[1]Stand Density Index, calculated in metric units (trees per ha).

[2]Crown bulk density (kg/m^3)

[3]Number of trees per hectare whose diameter at breast height (DBH) is less than 18 cm

[4]According to the Anderson rating system[4]

[5]Basal area in m^2 of all mountain hemlock (MHD) and white fir (WF) trees with DBH $> 46cm$.

[6]Pileburning slash involves removal of thinned trees only, while pileburning slash and fuels also involves removal of materials that were on the ground before thinning (Wall, Powers, 2012; personal communication)

≥ 87	> 0.037	> 49	$= 10$	> 7.5	Thin, pileburn slash and fuels, prescribed burn
				≤ 7.5	Thin, pileburn slash and fuels
			> 10	N/A	Thin, pileburn slash and fuels
			< 10	N/A	Thin, pileburn slash
		≤ 49	$= 10$	≥ 7.5	Prescribed burn
	≤ 0.037	N/A	$= 10$	≥ 7.5	Prescribed burn
N/A	N/A		$\in \{6, 8, 9, 10\}$	N/A	Prescribed burn[7]
Mixed conifer dry (MCD) plant association					
< 87	N/A	N/A	N/A	N/A	Prescribed burn
≥ 87	> 0.037	> 49	$\in \{10, 11\}$	N/A	Thin, pileburn slash and fuels, prescribed burn
			≥ 12	N/A	Thin, pileburn slash and fuels
			< 10	N/A	Thin, pileburn slash
		≤ 49	$\in \{10, 11\}$	N/A	Prescribed burn
	≤ 0.037	N/A	$\in \{10, 11\}$	N/A	Prescribed burn
N/A	N/A		$\in \{6, 8, 9, 10\}$	N/A	Prescribed burn[7]

---

[7]Only if prescribed burn was assigned in period 1 (applies to period 2 treatment assignments only)

Appendix C

INTER- AND INTRA-FRONTIER COMPARISON METRICS

This chapter describes in more detail the metrics used to compare the frontiers generated by solving the multi-objective model described in §1.2.7. The metrics are broken up into two groups. *Inter-frontier comparison metrics* are those metrics that quantify some feature of a frontier. That is, the metric has only a single value per frontier. These metrics may be used either alone or with other metrics to make comparisons at the frontier level. *Intra-frontier comparison metrics* are those metrics that quantify some feature within a frontier. There may be multiple values of this metric per frontier, depending on the metric and the number of objectives. These metrics may be used either alone or with other metrics to make comparisons at the objective (or ecosystem service) level.

C.1 Inter-Frontier Comparison Metrics

Researchers in the field of EMO develop algorithms to generate a set of non-dominated solutions that best represents the true Pareto-optimal frontier [21]. To test their algorithms, they solve a benchmark multi-objective optimization problem and compare their resulting frontiers to the known Pareto front for that problem [45]. There is no assurance of optimality of the solutions derived using these algorithms, so they require a means of comparing the resulting frontiers to determine if one algorithm produces a "better" non-dominated frontier than another. Zitzler et al. provide a review of comparison methods [80]. These methods aim to quantify certain traits about a frontier that can be used to measure their success in approximation of the true frontier.

When necessary, the normalization of the objective space is such that all objectives are maximized, and each frontier is contained within the unit hypercube. That is, each

objective is bounded between 0 and 1, yielding a frontier bounded by $[0,1]^N$. Defining the nadir solution $\mathbf{z}_{\mathrm{nad}}$ of a frontier of points $z \in Z$ as the objective vector with components

$$\mathbf{z}_{\mathrm{nad}}^i = \inf_z\{z^i\} \quad \forall 1 \le i \le N \tag{C.1}$$

and the ideal solution as the objective vector with components

$$\mathbf{z}_{\mathrm{ideal}}^i = \sup_z\{z^i\} \quad \forall 1 \le i \le N \tag{C.2}$$

then under my normalization, the nadir solution is the origin and the ideal solution is the N-dimensional vector of ones $\mathbf{1}_N$.

The definitions of dominance terms used here are in Table C.1.

Relation	Solutions		Frontiers	
Strictly dominates	$\mathbf{z}_1 \succ\succ \mathbf{z}_2$	$\mathbf{z}_1$ is better than $\mathbf{z}_2$ in all objectives	$Z_1 \succ\succ Z_2$	Every solution in Z_2 is strictly dominated by at least one solution in Z_1
Dominates	$\mathbf{z}_1 \succ \mathbf{z}_2$	$\mathbf{z}_1$ is better than $\mathbf{z}_2$ in at least one objective and is not worse in any objective	$Z_1 \succ Z_2$	Every solution in Z_2 is dominated by at least one solution in Z_1
Better			$Z_1 \rhd Z_2$	Every solution in Z_2 is weakly dominated by at least one solution in Z_1 and $Z_1 \neq Z_2$
Weakly dominates	$\mathbf{z}_1 \succeq \mathbf{z}_2$	$\mathbf{z}_1$ is at least as good as $\mathbf{z}_2$ in all objectives	$Z_1 \succeq Z_2$	Every solution in Z_2 is weakly dominated by at least one solution in Z_1
Incomparable	$\mathbf{z}_1||\mathbf{z}_2$	Neither $\mathbf{z}_1$ nor $\mathbf{z}_2$ weakly dominates the other	$Z_1||Z_2$	Neither Z_1 nor Z_2 weakly dominates the other

Table C.1: Definitions of dominance relationships between solutions and between frontiers, reproduced from Zitzler *et al.* [80].

C.1.1   Additive binary epsilon indicator $I_{\epsilon+2}$

Given two frontiers, Z_1 and Z_2, the additive binary epsilon indicator is defined as [80]

$$I_{\epsilon+2}(Z_1, Z_2) = \inf_{\epsilon \in \mathbb{R}} \left\{ \forall \mathbf{z}_2 \in Z_2 \; \exists \mathbf{z}_1 \in Z_1 : \mathbf{z}_1 \succeq_{\epsilon+} \mathbf{z}_2 \right\} \tag{C.3}$$

where $\succeq_{\epsilon+}$ is the additive ϵ-dominance relationship:

$$\mathbf{z}_1 \succeq_{\epsilon+} \mathbf{z}_2 \iff \epsilon + \mathbf{z}_1^i \geq \mathbf{z}_2^i \quad \forall 1 \leq i \leq N \tag{C.4}$$

Intuitively, ϵ is the minimum amount by which a frontier Z_1 must be translated such that every solution $\mathbf{z}_2 \in Z_2$ is "covered". See Figure C.1. Positive values of $I_{\epsilon+2}(Z_1, Z_2)$ indicate the presence of points $\mathbf{z}_2 \in Z_2$ that are not dominated by Z_1. Negative values of $I_{\epsilon+2}(Z_1, Z_2)$ indicate that Z_1 strictly dominates Z_2 ($Z_1 \succ\succ Z_2$).
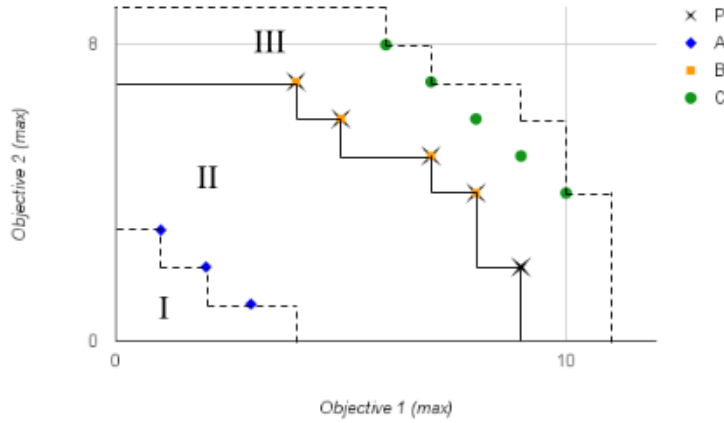

Figure C.1: Depiction of the additive binary epsilon indicator $I_{\epsilon+2}$ and the additive epsilon dominance relationship $\succeq_{\epsilon+}$. In the figure,

$$I_{\epsilon+2}(P, A) = -4 < 0 \qquad I_{\epsilon+2}(P, B) = 0 \qquad I_{\epsilon+2}(P, C) = 2 > 0$$

Region III is ϵ_+-dominated for $\epsilon = 2$; region II is ϵ_+-dominated for $\epsilon = 0$; region I is ϵ_+-dominated for $\epsilon = -4$. Note that region II also encompasses region I, and region III encompasses region II.

C.1.2   Additive unary epsilon indicator $I_{\epsilon+}$

I define the unary epsilon indicator as

$$I_{\epsilon+}(Z) = I_{\epsilon+2}(Z, \mathbf{z}_{\text{ideal}}) \tag{C.5}$$

That is, the additive unary epsilon indicator is identical to the additive binary epsilon indicator where the second frontier consists of a single point: the ideal solution for the first frontier.

This differs from the unary epsilon indicator traditionally used in EMO [80]. In EMO, the frontier is compared against a reference nondominated set. However, because the frontiers in the present study have guaranteed optimality, there is no reference set against which to compare them.

C.1.3   Unary hypervolume indicator I_{H1} and binary hypervolume indicator I_{H2}

For every solution $\mathbf{z}_i$ in a frontier Z define the hyperrectangle r_i whose diagonal corners are the origin and the objective vector $\mathbf{z}_i = \langle z^1, \ldots, z^N \rangle$ (see Figure C.2). Then the unary hypervolume indicator of the frontier Z is the N-dimensional volume of the union of all of the hyperrectangles corresponding to the solutions in Z:

$$I_{H1}(Z) = \text{vol}\left(\bigcup_{i=1}^{|Z|} r_i \right) \tag{C.6}$$

Then define the binary hypervolume indicator of two frontiers Z_1 and Z_2 as [79]

$$I_{H2}(Z_1, Z_2) = I_{H1}(Z_1 + Z_2) - I_{H1}(Z_2) \tag{C.7}$$

where $I_{H1}(Z_1 + Z_2)$ is the unary hypervolume indicator of the frontier consisting of the nondominated points in $Z = \{z \in Z_1 \cup Z_2\}$. See Figure C.3. The binary hypervolume indicator provides the volume of frontier Z_1 that is not contained within frontier Z_2. Larger values of I_{H1} correspond to frontiers occupying larger amounts of the objective space. In a
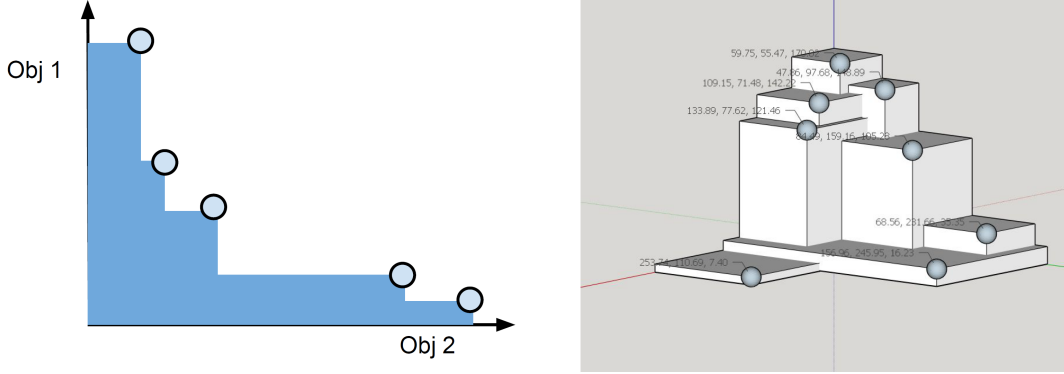
Figure C.2: Depiction of the hypervolumes of frontiers with two objectives (left) and three objectives (right).

normalized objective space, $I_{H2}(Z_1, Z_2) > I_{H2}(Z_2, Z_1)$ indicates areas of less conflict between objectives in Z_1 than in Z_2.

I developed a custom algorithm to solve for the hypervolume idicators. The details of the algorithm may be found in §A.

C.1.4 Unary distance indicator I_d

The unary distance indicator measures the average distance from the frontier to the ideal solution:

$$I_d = \frac{\sum_{\mathbf{z} \in Z} ||\mathbf{z}_{\text{ideal}} - \mathbf{z}||}{N} \tag{C.8}$$

Smaller values of I_d correspond to frontiers that are closer to the ideal solution, which may imply less conflict between objectives. This metric is analogous to the unary distance indicator more commonly used in EMO [19]. Where the metric used here measures the distance to the ideal solution, the traditional metric measures the distance to a reference Pareto frontier.
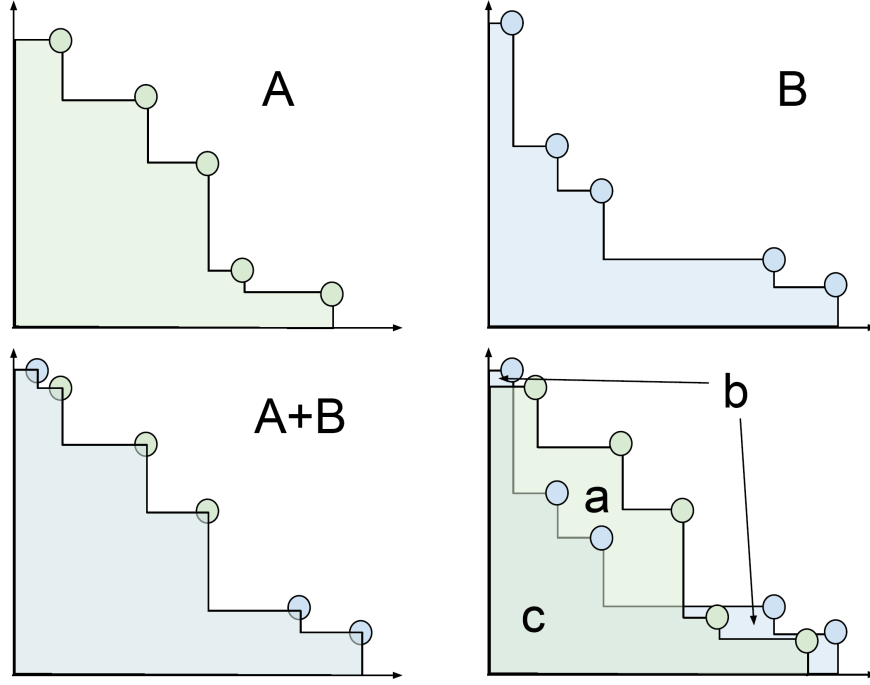
Figure C.3: Depiction of the binary hypervolume indicator. The individual frontiers are shown in the top row: frontier A (left) and frontier B (right). The merged frontier $A + B$ is shown in bottom left - note the absence of points that were dominated when combined. Following the naming of regions as shown in the bottom right figure, the binary hypervolume indicator is equal to

$$I_{H2}(A, B) = (\text{area}_a + \text{area}_b + \text{area}_c) - (\text{area}_b + \text{area}_c) = \text{area}_a$$

C.1.5 Unary Spacing Indicator I_s

The unary spacing indicator, or Schott's spacing metric [63], computes the standard deviation of the distance between points in the frontier:

$$I_s = \sqrt{\frac{1}{N-1} \sum_{\mathbf{z} \in Z} (d_z - \bar{d})^2} \tag{C.9}$$

where

$$d_z = \min_{\mathbf{y} \in Z, \mathbf{y} \neq \mathbf{z}} ||\mathbf{z} - \mathbf{y}|| \tag{C.10}$$

and $\bar{d}$ is the average over all d_z. In EMO, the spacing indicator provides a measure of an algorithm's ability to search the frontier space uniformly. Here, the spacing metric provides a measure of the flexibility afforded to the decision maker under each climate scenario, since smaller values of I_s imply a higher density of solutions and greater flexibility.

C.2 Intra-Frontier Comparison Metrics

While the above methods provide frontier-level metrics of conflict and tradeoffs, there are two methods employed here to also determine the degree of conflict within a single frontier. The first is an approach used in many-objective optimization, and the second is a variant of the unary hypervolume indicator.

C.2.1 Pearson correlation coefficients

Given the increased difficulty in solving many-objective optimization problems [44], researchers in this field seek to reduce the number of objectives considered in the model. To determine which objectives most strongly influence the shape of the frontier, they compute the correlation between each pair of objectives [23]. Objective pairs with strong negative correlation conflict with one another. The Pearson correlation coefficients are computed per

$$\rho_{X,Y} = \frac{\text{cov}(X,Y)}{\sigma(X)\sigma(Y)} \tag{C.11}$$

where, for objectives x and y, X and Y are

$$X = \{\mathbf{z}_1^x, \mathbf{z}_2^x, \ldots, \mathbf{z}_{|Z|}^x\} \tag{C.12}$$

$$Y = \{\mathbf{z}_1^y, \mathbf{z}_2^y, \ldots, \mathbf{z}_{|Z|}^y\} \tag{C.13}$$

C.2.2 Area of 2D frontier projection A_{xy}

The second intra-frontier comparison metric uses the unary hypervolume indicator described in §C.1.3. Given a frontier with objective vectors in N dimensions, take two objectives x and y, and project the N-dimensional frontier to the two-dimensional xy-plane. Remove

solutions dominated in this projection, and compute the hypervolume indicator (which, in two-dimensions, is simply the area). See Figure C.4. Larger values of A_{xy} imply less conflict between objectives x and y.
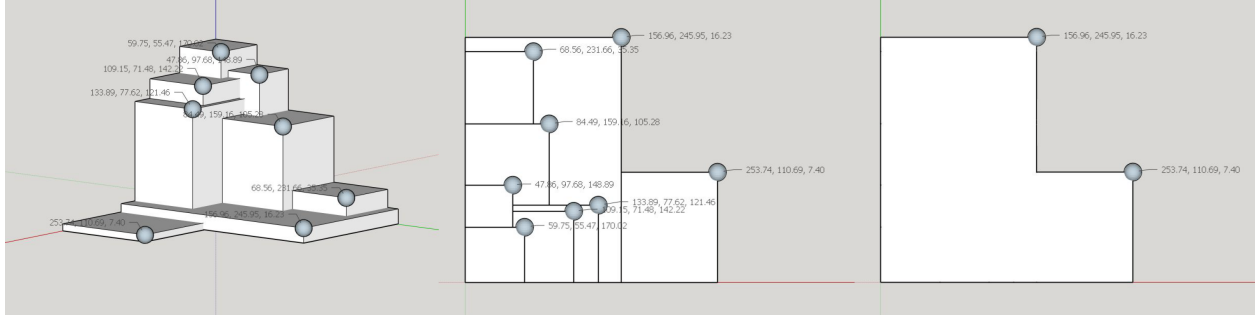

Figure C.4: Comparing conflict between objectives based on the area bounded by two-dimensional frontier projection. Left is the original frontier; middle shows the 2D projection of the frontier; right shows the projected frontier with all dominated solutions removed. Assuming both objectives are maximized, the larger the area bounded by the cross-sectional area, the less conflict between the objectives.